ACKNOWLEDGMENT

The authors are grateful to some of their associates for helpful information, notably T. C. Hana and H. M. Heinemann. Also they are grateful to the IEEE reviewers who offered a correction to the first manuscript. In addition to the credited references, it is notable that the bulletins from suppliers show a steady trend toward complete and reliable information; we would urge that the MKS units be standardized for all purposes. Future bulletins might well include the TDQ as a significant property of an insulating material, especially if intended for high-frequency applications with high power density.

REFERENCES

[1] "Properties of solid insulating materials," *Gen. Radio Experimenter*, vol. 14, no. 1, pp. 6–7, June 1939. (Dielectric and thermal.)
[2] *American Institute of Physics Handbook*, 2nd ed, 1963. (Thermal conductivity, R. L. Powell, pp. 4-76–4-101.)
[3] G. A. Slack, "Thermal conductivity of silicon, silicon carbide and diamond," *J. Appl. Phys*, vol. 35, pp. 3460–3466, Dec. 1964.
[4] Chemical Rubber Co., *Handbook of Chemistry and Physics*, 48th ed., 1967. (Thermal conductivity, pp. E-2–E-11.)
[5] A. S. Grove, *Physics and Technology of Semiconductor Devices*. New York: Wiley, 1967. (Dielectric and thermal properties of materials.)
[6] R. C. Levine, "Determination of thermal conductance of dielectric-filled strip transmission line from characteristic impedance," *IEEE Trans. Microwave Theory Tech.*, vol. MTT-15, pp. 645–646, Nov. 1967. (One relation between thermal and electrical properties. Not MKS units.)
[7] ITT, *Reference Data for Radio Engineers*, 5th ed, 1968.
[8] G. Klein, "Thermal resistivity table simplifies temperature calculations," *Microwaves*, vol. 9, no. 2, pp. 58–59, Feb. 1970. (Confusion by use of inverse conductivity and various units other than MKS.)
[9] C. A. Harper, Ed., *Handbook of Materials and Processes for Electronics*. New York: McGraw-Hill, 1970. (Dielectric and thermal properties.)
[10] L. I. Maissel and R. Glany Eds., *Handbook of Thin Film Technology* New York: McGraw-Hill, 1970. (Dielectric and thermal properties of substrate materials.)
[11] "1972 materials selector, " *Materials Eng.*, vol. 74, no. 4, Sept. 1971. (Excellent tables.)
[12] R. L. Powell, correspondence, NBS survey on thermal conductivity; 1972. (Diamond, silicon, other crystals.)
[13] M. Neuberger, *Handbook of Electronic Materials, Vol. 5, Group IV Semiconducting Materials*. New York: Plenum, 1971. (Diamond, germanium, silicon, silicon carbide.)

Planar Broad-Band 180° Hybrid Power Divider/Combiner Circuit

MAHESH KUMAR, MEMBER, IEEE, RAYMOND J. MENNA, MEMBER, IEEE, AND HO-CHUNG HUANG, SENIOR MEMBER, IEEE

***Abstract*—A planar broad-band 180° hybrid is presented. The hybrid is realized using a 3-dB 90° hybrid and a 0-dB 90° tandem hybrid. An interdigitated version of the hybrid fabricated on alumina substrate performed well over the 4–8-GHz band. The hybrid has an insertion loss of 0.5 dB, phase imbalance of ±7°, and an isolation of better than 18 dB over the band.**

Manuscript received April 7, 1981; revised July 13, 1981 This work was supported by the Office of Naval Research, Arlington, VA, under Contract N00014-79-0568, and monitored by M. N. Yoder.

The authors are with RCA Laboratories, David Sarnoff Research Center, Princeton, NJ 08540.

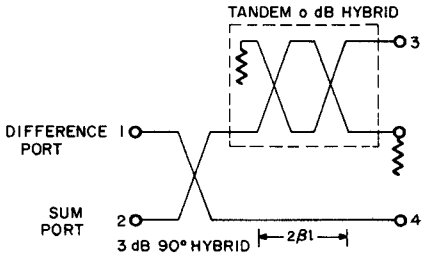

Fig. 1. Schematic of a 180° hybrid.

I. INTRODUCTION

In the past, 180° hybrids have been extensively used in balanced mixers, switching networks, phase shifters, and push–pull amplifiers. The recent interest in monolithic GaAs integrated circuits has opened the need for a 180° planar hybrid compatible to monolithic integration on GaAs substrates.

Conventional hybrid rings have been used as 180° hybrids. The hybrid ring has a narrow bandwidth. Reflection-type 180° hybrids have been reported in literature [1]. The problem with this kind of hybrid is the practical difficulty of realizing a good short or open circuit over wide band of frequencies. The commercially available 180° hybrids use a tandem connection of two couplers using broadside coupling [2], [3]. This is a multilayer structure and can be realized using striplines only. Recently, a 3-dB 180° hybrid has been reported [4] which uses a slot line–microstrip coupling. The abovementioned structures for 180° hybrids are not planar, and not easily compatible to monolithic circuit fabrication

This paper presents an analysis and experimental results of a broad-band 180° planar hybrid. This hybrid is a four-port device with two input ports and two output ports. One of the input ports is designated as the sum port and the other as the difference port. A signal fed into the sum port or the difference port is divided into two signals of equal amplitude with a phase difference of 0° or 180°, respectively. This hybrid has been realized using a 3-dB interdigitated, 3-dB 90° hybrid, and a 0-dB 90° interdigitated tandem hybrid. The latter hybrid introduces an additional 90° phase shift which is independent of frequency. The analysis of the circuit is presented in Section II. The hybrid has been designed and fabricated on alumina substrate for *C*-band operation. The experimental results are presented in Section III.

II. ANALYSIS OF THE HYBRID

The schematic of the hybrid is shown in Fig. 1. It is a four-port device. Ports 1 and 2 are the input ports and ports 3 and 4 are the output ports. When the signal is fed to port 1, the signals appearing at port 3 and port 4 are both 3 dB below the input signal and have a phase difference of 180°. When a signal is fed at port 2, the signals appearing at ports 3 and 4 are both 3 dB below the input signal and are in phase. These two cases are considered separately and the analysis is presented for both cases.

Case 1: Input at Difference Port

Let θ be the coupling angle and l be the coupling length. The hybrid is illustrated in Fig. 1. Port 4 has an extra length of transmission line of length $2\beta l$. It will be shown later that the phase difference of the two output signals appearing at ports 3 and 4 is independent of frequency. Assume that a unit amplitude signal is fed at port 1 (port 2 is theoretically isolated), then the

0018-9480/81/1100-1233$00.75 ©1981 IEEE

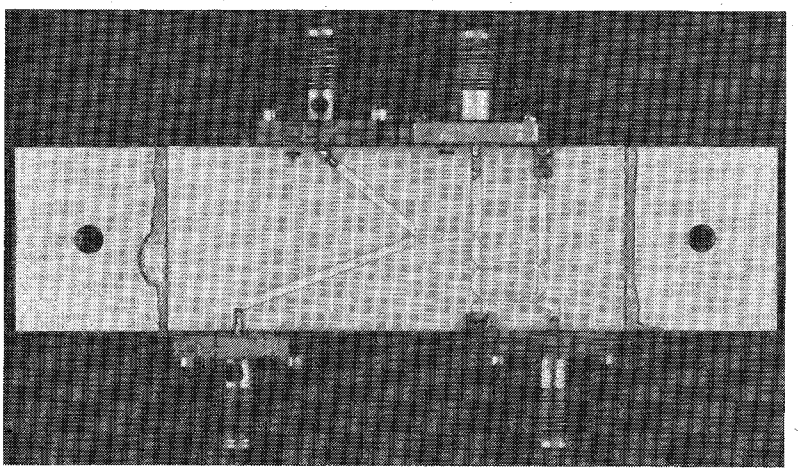

Fig. 2. Photograph of the hybrid.

signals appearing at port 3, 4, and I can be obtained as

$$\text{Signal at port 3, } V_3 = -\sin\theta \sin^2\theta\, e^{-j3\beta l} \quad (1)$$

$$\text{Signal at port 4, } V_4 = \cos\theta\, e^{-j3\beta l} \quad (2)$$

$$\text{Signal at port } I, \; V_I = j \sin\theta \cos 2\theta\, e^{-j3\beta l}. \quad (3)$$

For $\theta = \pi/4$ at band center, for a 3-dB hybrid, (1)–(3) become

$$V_3 = -0.707\, e^{-j3\beta l} \quad (4)$$

$$V_4 = 0.707\, e^{-j3\beta l} \quad (5)$$

$$V_I = 0. \quad (6)$$

Thus the signals appearing at ports 3 and 4 have a phase difference of 180° and are equal in magnitude which is $\sqrt{2}$ below the input signal (3 dB below in power). Port I is an isolated port since the signal appearing at port I is zero.

Case 2: Input at Sum Port

In this case, the signal is fed at port 2 (Fig. 1) and port 1 is theoretically isolated. The signals appearing at ports 3, 4, and I can be obtained as

$$\text{Signal at port 3, } V_3 = j \cos\theta \sin 2\theta\, e^{-j3\beta l} \quad (7)$$

$$\text{Signal at port 4, } V_4 = j \sin\theta\, e^{-j3\beta l} \quad (8)$$

$$\text{Signal at port } I, \; V_I = \cos\theta \cos 2\theta\, e^{-j3\beta l}. \quad (9)$$

For $\theta = \pi/4$ at band center, for a 3-dB hybrid, (7)–(9) become

$$V_3 = j\, 0.707\, e^{-j3\beta l} \quad (10)$$

$$V_4 = j\, 0.707\, e^{-j3\beta l} \quad (11)$$

$$V_I = 0. \quad (12)$$

Thus signals appearing at ports 3 and 4 are in phase having equal amplitude each 3 dB below the input power. Port I is an isolated port and is match terminated.

In both cases, the phase difference between two output ports is independent of frequency. However, the amplitude is frequency dependent, since the coupling angle θ is frequency dependent. The bandwidth of the hybrid will be slightly less than the bandwidth of each 90° hybrid used. A 90° interdigitated hybrid has over an octave bandwidth.

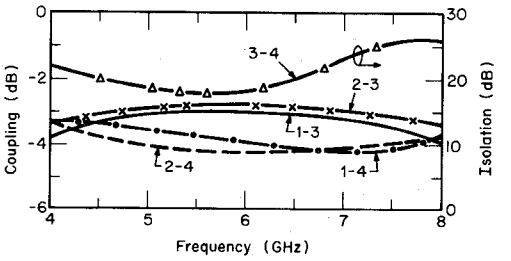

Fig. 3. Variation of coupling and isolation between different ports with frequency of the hybrid.

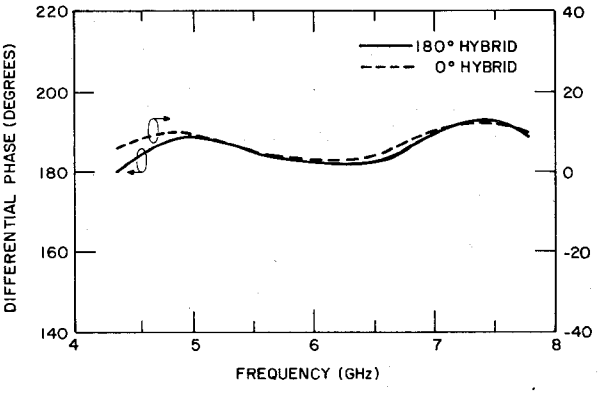

Fig. 4. Variation of differential phase with frequency for two cases of 180° and 0° hybrids.

III. Experimental Results

The hybrid shown in Fig. 1 consists of three 3-dB 90° hybrids. The design of an interdigitated, 90° hybrid is done using the well-documented theory [6], [7]. We have fabricated this hybrid on a 25-mil-thick alumina substrate. The photograph of the hybrid is shown in Fig. 2. Fig. 3 shows the coupling between different ports of the hybrid. The isolation between two output ports is better than 18 dB. The powers of the two output ports differ by less than 1.5 dB and the insertion loss of the hybrid is less than 0.5 dB over the 4–8-GHz band. The variation of the phase with frequency is presented in Fig. 4, for both cases, when the signal is fed at the different ports or sum port, resulting in two output signals which are 180° out of phase or in phase, respectively. The maximum VSWR at the different ports is 1.4 over the band.

IV. Conclusions

We have presented an analysis and experimental results of a 180° hybrid. This hybrid has been realized on alumina substrate. It has a bandwidth of 3 GHz over the 4–8-GHz band with a loss of 0.5 dB, an isolation of >18 dB, and a phase unbalance of ±7°. The hybrid reported here is compatible to monolithic integration on GaAs substrates.

References

[1] H. Seidel, "Hybrid coupled amplifier," U. S. Patent 3 423 688, Jan. 21, 1969.

[2] H. J Hindin and A Rosenzweig, "3-dB couplers constructed from two tandem connected 8.34 dB asymmetric couplers," *IEEE Trans. Microwave Theory Tech.*, vol. MTT-16, no. 2, pp. 125–126, Feb. 1968.

[3] J P. Shelton, J. Wolfe, and R. C Van Wagoner, "Tandem couplers and phase shifters for multi-octave bandwidths," *Microwaves*, vol. 4, pp. 14–19, Apr 1965.

[4] G. Lennart Nystrom, "Synthesis of broadband 3-dB hybrids based on the two-way power divider," *IEEE Trans. Microwave Theory Tech.*, vol. MTT-29, no. 3, pp. 189–194, Mar. 1981.

[5] W. S Metcalf, "Cascading 4-port networks," *Microwave J.*, vol. 12, pp. 77–82, Sept. 1969.

[6] P. O. Wer, "Design equations for an interdigitated directional coupler," *IEEE Trans. Microwave Theory Tech.*, vol. MTT-23, pp. 253–255, Feb. 1975.

[7] A. Presser, "Interdigitated microstrip coupler design," *IEEE Trans. Microwave Theory Tech.* vol. MTT-26, no. 10, pp. 801–806, Oct. 1978.

An Empirical Relationship for Electromagnetic Energy Absorption in Man for Near-Field Exposure Conditions

I. CHATTERJEE, M. J. HAGMANN, AND O. P. GANDHI

***Abstract*—An empirical relationship is presented for the whole-body-average electromagnetic energy absorption in a 180-cell block model of man for near-field exposure conditions. Consideration is restricted to near fields with *P* polarization (no component of *E* directed arm-to-arm) in which the magnitude of the incident electric field is maximum immediately in front of the abdominal region. A highlight of this work is the considerably reduced whole-body average energy absorption for near-field partial-body exposures as compared to that obtained under plane-wave irradiation conditions.**

I. Introduction

The plane-wave spectrum approach [1] has previously been used [2] to calculate the mass-normalized electromagnetic energy absorption (specific absorption rate or SAR) and its distribution for prescribed near-field exposure conditions. This method is particularly suited for leakage-type near fields such as those from RF heat sealers and other electronic equipment where the coupling back to the source may be neglected. For the numerical calculations, a 180-cell block model of the 50th percentile man [3] has been used.

The procedure developed previously can be used for any incident fields with tangential components prescribed over a plane. We have restricted most of our calculations to fields prescribed over a vertical plane just in front of the feet of the block model. Since the fields emanating from many localized sources are likely to roll off monotonically to negligible values in the two dimensions of the plane, the calculations have been performed for prescribed electric fields having a half-cycle cosine variation along both the vertical and horizontal axes. For several test cases, it has been shown that such approximated fields give whole-body SAR's that are within 5–10 percent of the values that would have been obtained from exactly prescribed fields, [2]. For each set of prescribed fields, the remaining field components (body-normal $\boldsymbol{E}$ component and $\boldsymbol{H}$) may be obtained from Maxwell's equations.

The phase variation of the prescribed fields is important for exact calculations of SAR. It has, however, been shown [2] that the worst case (maximum whole-body SAR) is always obtained for constant phase in the prescribed fields. We have assumed no phase variation in the prescribed fields in order to avoid the need for phase measurements and thereby have obtained an upper bound for values of whole-body SAR. Since the whole-body SAR would also be a function of the height of the maximum of the prescribed E-field relative to the block model, various placements have been considered. Except at frequencies corresponding to strong part-body resonances, the condition for maximum whole-body SAR corresponds to the case where the peak of the prescribed field is located in front of the abdominal region. Consequently the empirical equation is applied for this placement for different values of physical extent of the assumed vertical electric fields, the accompanying $\boldsymbol{E}$ and $\boldsymbol{H}$ components being given by Maxwell's equations. We have considered only P polarization (no component of $\boldsymbol{E}$ directed arm-to-arm) for the prescribed fields since it produces greater absorption than N polarization ($\boldsymbol{E}$ arm-to-arm) at frequencies below 300 MHz [4]. Also, for currently encountered RF sealers identified as sources of significant leakage fields [5],[6], the vertical component of $\boldsymbol{E}$ (E_v) is much larger than the horizontal component (E_h). It is recognized that the SAR due to E_h may be comparable to that due to E_v for frequencies above 300 MHz. For these frequencies, the contribution of E_h to the SAR should also be included in the calculations for near-field electromagnetic energy absorption. Nevertheless, there are a number of applications where the vertical component E_v may indeed be much larger than the arm-to-arm directed field E_h. The empirical equation is useful for such cases even at frequencies above 300 MHz.

II. Effect of Placement of the Body Relative to Fields

As previously mentioned, whole-body SAR is a function of the height of the maximum of the prescribed E fields relative to the block model. Calculations of SAR were made for assumed half-cycle cosine variations with $\Delta_v = 0.2\ \lambda$ and $\Delta_h = 0.5\ \lambda$, where Δ_v and Δ_h are, respectively, the vertical and horizontal widths of the best fit half-cycle cosine functions to the prescribed leakage fields, and λ is the free-space wavelength. These results are given in Table I for various relative placements of the fields and the body for four different frequencies. The frequencies in Table I were selected to correspond to those used for RF heat sealers and to resonant frequencies for the whole body, the arm, and the head [7], [8]. The physical extents Δ_v and Δ_h of the fields were taken to be similar to those commonly encountered for RF sealers. From Table I one can see that the condition for maximum whole-body

Manuscript received March 25, 1981; revised June 29, 1981. This work was supported by the National Institute of Environmental Health Sciences, Research Triangle Park, NC, under Grant ES02304.

The authors are with the Department of Electrical Engineering, University of Utah, Salt Lake City, UT 84112

0018-9480/81/1100-1235$00.75 ©1981 IEEE